ISSN 1560-8034, 1605-6582 (On-line), SPQEO, 2019. V. 22, N 2. P. 165-170.

Effect of ultrasound irradiation on the electro-physical properties of the structure of $Al–Al_2O_3–CdTe$

A.K. Uteniyazov, K.A. Ismailov

Berdakh Karakalpak State University
Uzbekistan, Republic of Karakalpakstan, 742012 Nukus, Abdirov str., 1
E-mail: abat-62@mail.ru

Abstract. It has been shown that the density of surface states at the interface of the $Al–Al_2O_3$–*p*-CdTe–Mo structure is sufficiently low. It was found that at the interface being in the thermodynamically equilibrium state, there is a bend of the edge of the allowed bands, as evidenced by the values of the surface potential, which are equal to 0.17 eV before and 0.25 eV after treatment. It has been ascertained that the surface states in the lower half of the band gap are almost completely annealed. It has been shown that ultrasonic treatment significantly affects the fluctuations of surface charges at the interface and eliminates unstable point defects located in the surface layer of semiconductor. It has been established that the ultrasonic treatment has practically no effect on the patterns of current transfer both in the forward and reverse directions. It has been shown that after the ultrasonic treatment, the forward current increases by about 25…30%, and the reverse current decreases by 6…9%, the rectification coefficient increases by 1.4 times.

Keywords: ultrasonic treatment, film, Schottky barrier, diode structure.

https://doi.org/10.15407/spqeo22.02.165
PACS 72.10.-d, 73.61.Ga, 73.40.Sx

Manuscript received 05.03.19; revised version received 16.05.19; accepted for publication 19.06.19; published online 27.06.19.

1. Introduction

Currently, it is considered as an established fact that ultrasonic treatment (UST) affects structural defects and the electrophysical characteristics of semiconductors and semiconductor structures [1-6]. The advantages of UST as compared with an annealing and radiation exposure include the following features:

1) the absorption of ultrasonic waves in a solid occurs predominantly in areas of disturbances of the periodicity of its crystal lattice and, therefore, the ultrasonic effect is more local;

2) the use of ultrasonic waves of different polarization and type allows to increase the selectivity of influence;

3) by selecting the frequency of ultrasonic vibrations, it is possible to achieve resonant transformations in the defect subsystem.

It is known that the electrophysical and photoelectric properties of heterojunctions and MOS structures strongly depend on the properties of semiconductor surface. Since various surface effects directly affect the reliability and stability of virtually all types of semiconductor devices, the study of surface properties in physics of metal-dielectric-semiconductor (MOS) structures plays a great role in all semiconductor technology. In [7, 8], we investigated surface states at the interface of the $Al–Al_2O_3$–*p*-CdTe structure. In [9], it was shown that such a structure has the property of an injection photodetector and amplifies the primary photocurrent even in the absence of an external bias voltage.

The goal of this work was to study the effect of ultrasonic treatment on the electrical properties of the $Al–Al_2O_3$–*p*-CdTe structure, *i.e.*, MOS structure.

2. Samples and measurement method

To solve the problems posed, we obtained *p*-CdTe film structures with a columnar grain structure on a Mo substrate by sublimation in a hydrogen flow. A MOS structure was created on the surface of the obtained *p*-CdTe films by sputtering aluminum in vacuum ($\sim10^{-5}$ Torr) [10]. The *p*-CdTe films had the resistivity $\rho \approx 10^9…10^{11}$ Ohm·cm and the lifetime of minority electron carriers $\tau \sim 10^{-8}…10^{-7}$ s. The performed X-ray structural analysis showed [11, 12] that a thin oxide layer of Al_2O_3 with the thickness close to 30 nm is formed during the preparation process, but this layer plays a very important role in operation of the structure obtained.

© 2019, V. Lashkaryov Institute of Semiconductor Physics, National Academy of Sciences of Ukraine

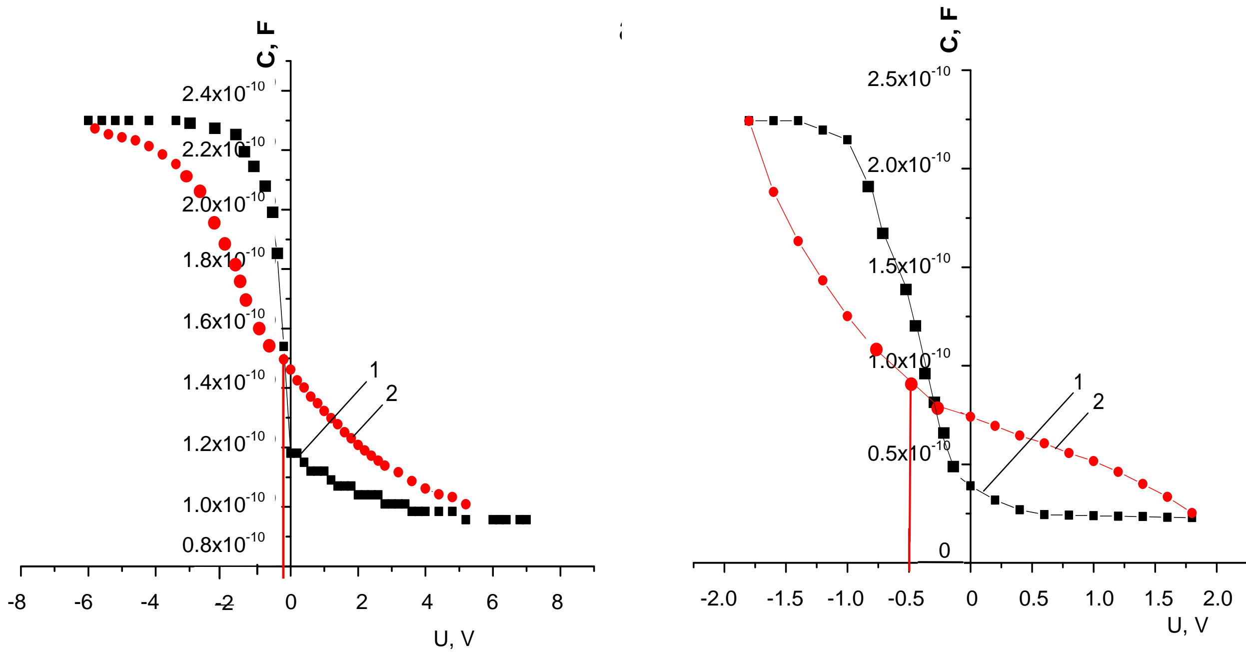

Fig. 1. The experimental (*1*) and calculated (*2*) *C*(*U*) curves for the structure Al–Al_2O_3–*p*-CdTe–Mo before (a) and after (b) UST.

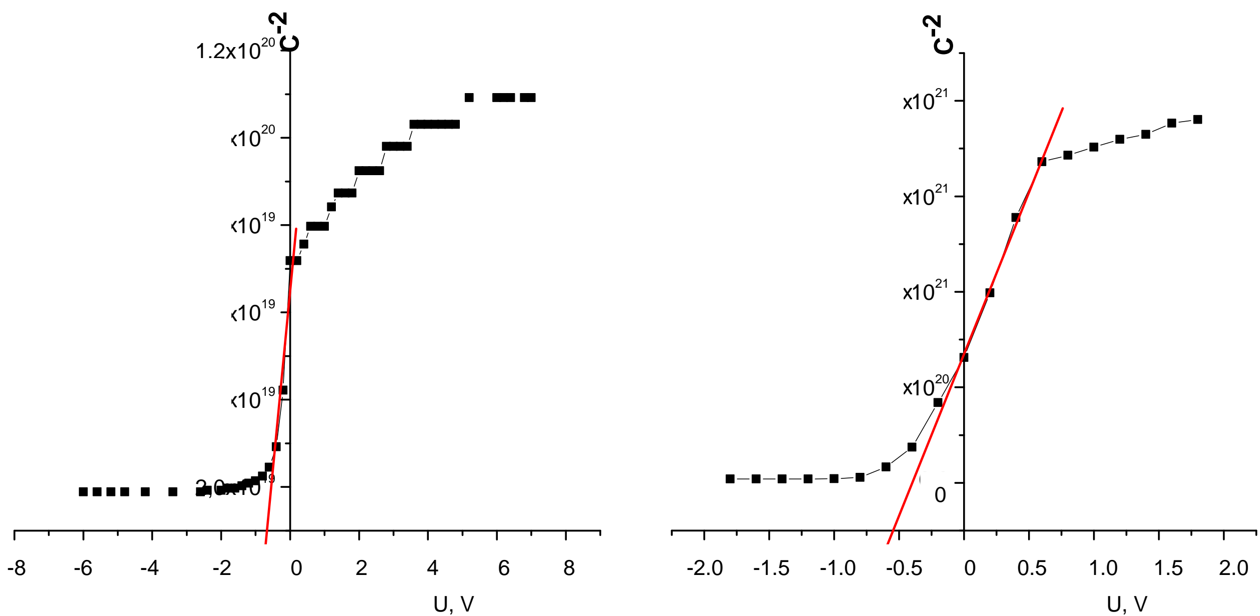

Fig. 2. Dependence of C^{-2}(*U*) of the structure of Al–Al_2O_3–*p*-CdTe–Mo before (a) and after (b) treatment.

Mainly due to this fact that it turns out not the metal-semiconductor structure, but the MOS structure, namely, Al–Al_2O_3–*p*-CdTe (Al – metal, Al_2O_3 – oxide, CdTe – semiconductor).

One of the methods for studying the surface of semiconductors in MIS (MOS) structures is the method of voltage-capacitance characteristics, which is non-destructive and a most informative. The capacitance-voltage characteristics were measured at the frequencies 1…5 kHz, which also made it possible to detect the presence of MOS elements (structures) in the samples under study. Ultrasonic treatment was carried out at the frequency 2.5 MHz with the power P = 1 W/cm^2 for 15 min.

3. Experimental results and discussion

The experimental voltage-capacitance characteristic (Fig. 1a, curve *1*) was taken at the frequencies within the kHz range. The calculated *C*(*U*) characteristic (Fig. 1a, curve *2*) was obtained like to that in [13]. When

determining the calculated $C(U)$ characteristics, we used the values of the oxide layer capacitance (C_i) and the concentration of equilibrium holes of semiconductor (p_0), determined directly from the experimental capacitance-voltage characteristic. The capacitance $C_i \approx 2.3 \cdot 10^{-10}$ F before and $C_i \approx 2.24 \cdot 10^{-10}$ F after UST was determined from the capacitance value on the plateau of the experimental $C(U)$ characteristics.

Having plotted $C(U)$ characteristics in coordinates $1/C^2(U)$ (see Figs. 2a, 2b), we determined the concentration of equilibrium hole carriers in the base of the structure, which turned out to be $\approx 2.85 \cdot 10^{13}$ cm^{-3} before and $1.9 \cdot 10^{12}$ cm^{-3} after UST. The concentration p_0 was also determined from the minimum capacitance $C_{\min}$, which was $\approx 3 \cdot 10^{13}$ cm^{-3} before and $2 \cdot 10^{12}$ cm^{-3} after UST.

Thus, the values of p_0 before and after treatment, determined by two independent methods, were almost at the same level.

In addition, extrapolating the $C(U)$ dependence to the voltage axis at $1/C^2 \to 0$, we determined the potential barrier height ~0.68 eV before and ~0.55 eV after UST. A comparison of the experimental capacitance-voltage characteristics before and after UST indicates that the capacitance of the structure, as a result of treatment, changes in a complex way.

First, the range of changes in the value of capacitance expands significantly, it is approximately four times larger. Second, the values of the bias voltage of the intersection point of the experimental and calculated $C(U)$ curves vary considerably; if they intersect at $U \approx 0.2$ V before treatment, then after at $U \approx$ ≈ 0.5 V. If we assume that the intersection point of $C(U)$ curves shows formation of flat bands at the interface between the semiconductor and dielectric (oxide), then it should be noted that UST has a significant effect on the surface potential ψ_S under thermodynamic equilibrium. It can be concluded that, at the interface of the MOS structure under study, the surface potential has a positive value, which significantly increases as a result of ultrasonic treatment. It means that the surface states are annealed in the lower half of the forbidden band of semiconductor. Comparison of the $1/C^2(U)$ dependences before and after treatment (see Figs 2a and 2b) also shows that in this structure the semiconductor surface at the interface before treatment has a certain region of depth inhomogeneities, which in the experiment appear as the ranges where the value $1/C^2$ remains constant in voltage, and each this range corresponds to a certain concentration of carriers in the depletion region, and they are practically absent after treatment. These experimental facts indicate the presence of micro-inhomogeneities in the depth of the semiconductor at the interface formed during formation of the MOS structure, which almost disappear after treatment. The density of the surface states of D_{it} was determined directly from the experimental high-frequency capacitance-voltage characteristic [14]. Charges on surface states at high frequencies ($\omega\tau >> 1$) have no time to follow the changes in the alternating voltage. At the same time, the capacitance of the MOS structure is described as that of the ideal MOS structure like to [14]:

$$C = \frac{C_i C_D}{C_i + C_D} \qquad (\text{F/cm}^2)\,, \tag{1}$$

where C_D is the semiconductor capacitance, C_i – capacitance of the dielectric layer (oxide), which is determined using $C(U)$ characteristics. Eq. (1) corresponds to the series connection of the semiconductor capacitance C_D and that of dielectric layer C_i. The semiconductor capacitance C_D changes with the voltage applied to the structure and is described by the following expression [14]:

$$C_D = \frac{dQ_S}{d\psi_S} = \frac{\varepsilon_S}{\sqrt{2} L_D} \frac{1 - e^{-\beta\psi_S} + \left(\dfrac{n_{p_0}}{p_{p_0}}\right)\left(e^{\beta\psi_S} - 1\right)}{F\left(\beta\psi_S, \dfrac{n_{p_0}}{p_{p_0}}\right)} \qquad (\text{F/cm}^2), \tag{2}$$

where L_D is the Debye length, ψ_S – surface potential, $\beta = q/kT$, k – Boltzmann constant.

Surface states affect the shape of the capacitance-voltage characteristic by shifting and stretching it along the stress axis. In the presence of a bound surface charge, a corresponding increase in charge on the metal contact is required, which occurs when a constant potential (U) is applied, as compared to an ideal MOS structure, in order to achieve the same value of the surface potential. According to the shape of the high-frequency volt-farad characteristic, the density of surface states is defined according to the following expression [14]:

$$D_{it} = \frac{C_i}{q}\left[\left(d\psi_S/dV\right)^{-1} - 1\right] - \frac{C_D}{q} \qquad (\text{cm}^{-2}\,\text{eV}^{-1}). \tag{3}$$

To determine the density of surface states D_{it}, first, using the value of the total capacitance C in accord with the formula (2), we determined the differential capacitance of semiconductor C_D for a given value of the bias voltage U. Then, having built the dependence $\psi_S(U)$ (see Figs 3a, 3b), we determine the derivative $d\psi_S/dV$ by graphical differentiation like to that in [14], which is necessary to determine the density of surface states by using the formula (3).

Analysis of the data in Figs. 3a and 3b shows that, indeed, at the interface with thermodynamic equilibrium (in the absence of a bias voltage) there is a bend of the edge of the allowed bands, as evidenced by the values of the surface potential, which are $\psi_S \approx 0.17$ eV before and $\psi_S \approx 0.25$ eV after treatment. It means that UST, in fact, leads to annealing of the surface states in the lower half of the forbidden band of semiconductor at the interface, which also confirms the decrease in the height of the potential barrier as a result of treatment. The above results suggest that these surface states are involved in formation of a potential barrier, especially before

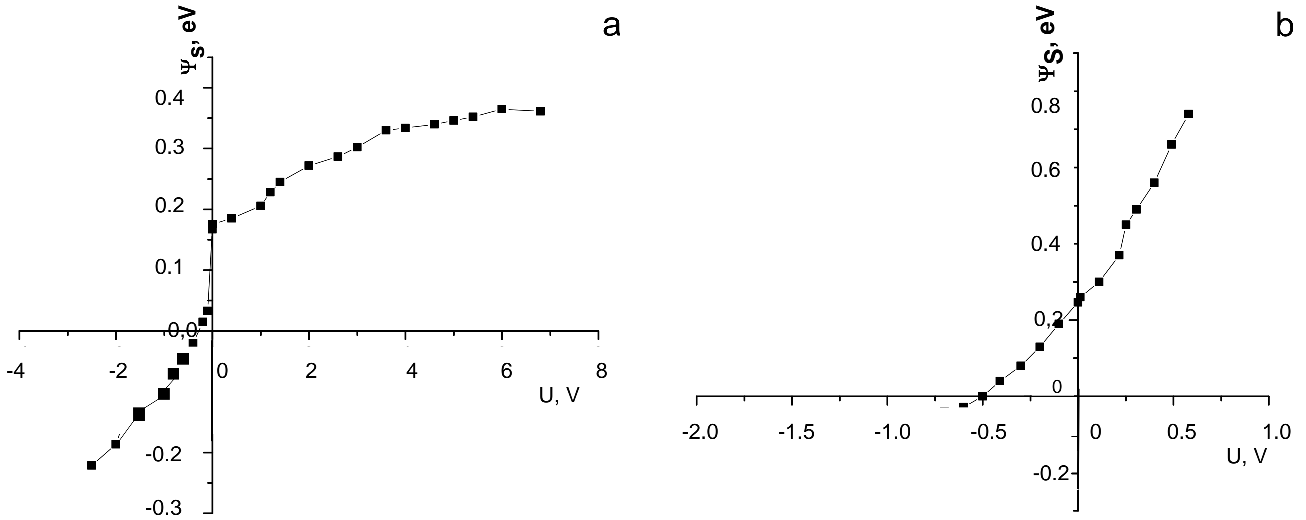

Fig. 3. The dependence of the surface potential ψ_S on the bias voltage U before (a) and after (b) treatment.

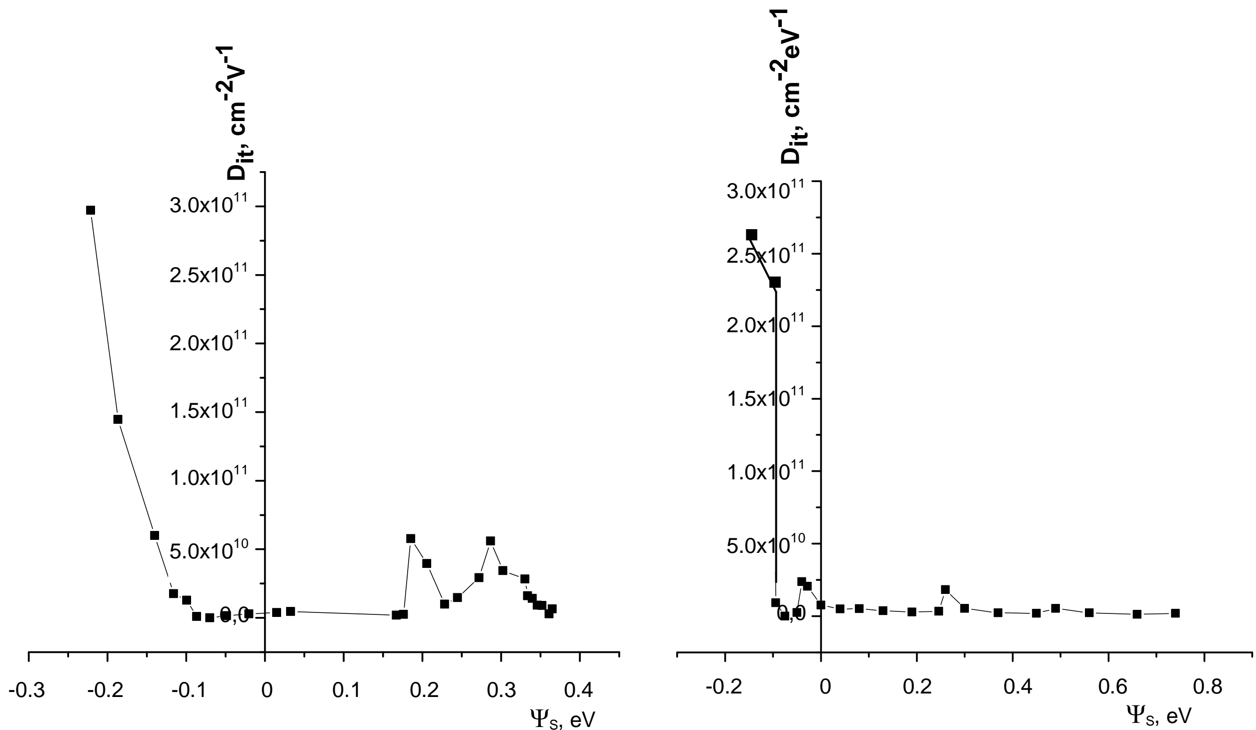

Fig. 4. The dependence of the effective density of surface states on the surface potential at the Al_2O_3–*p*-CdTe interface before (a) and after (b) UST.

treatment. After treatment, the surface potential reaches the value of strong inversion $\psi_S(\text{inv}) \approx 0.74$ eV, since the Fermi level is $E_F \approx 0.37$ eV, and $\psi_B \approx 0.37$ eV is the difference between the Fermi level and the position of the Fermi level in its own semiconductor E_i. It is known that with strong inversion the surface potential has the following analytical expression

$$\psi_S(\text{inv}) \approx (2kT/q)\ln(N_A/n_i). \quad (4)$$

Substituting the values $\psi_S(\text{inv}) \approx 0.74$ eV, $n_i \approx 3 \cdot 10^{13}$ cm^{-3} in the formula (4) – the intrinsic concentration of cubic modification of cadmium telluride and $T = 293$ K, we obtain the concentration of ionized acceptor centers $N_A \approx 2.4 \cdot 10^{12}$ cm^{-3}, which is almost equal to the concentration of equilibrium holes, determined from the curves of $1/C^2(U)$ dependences after treatment. It follows that UST almost completely anneals the surface states in the lower half of the semiconductor,

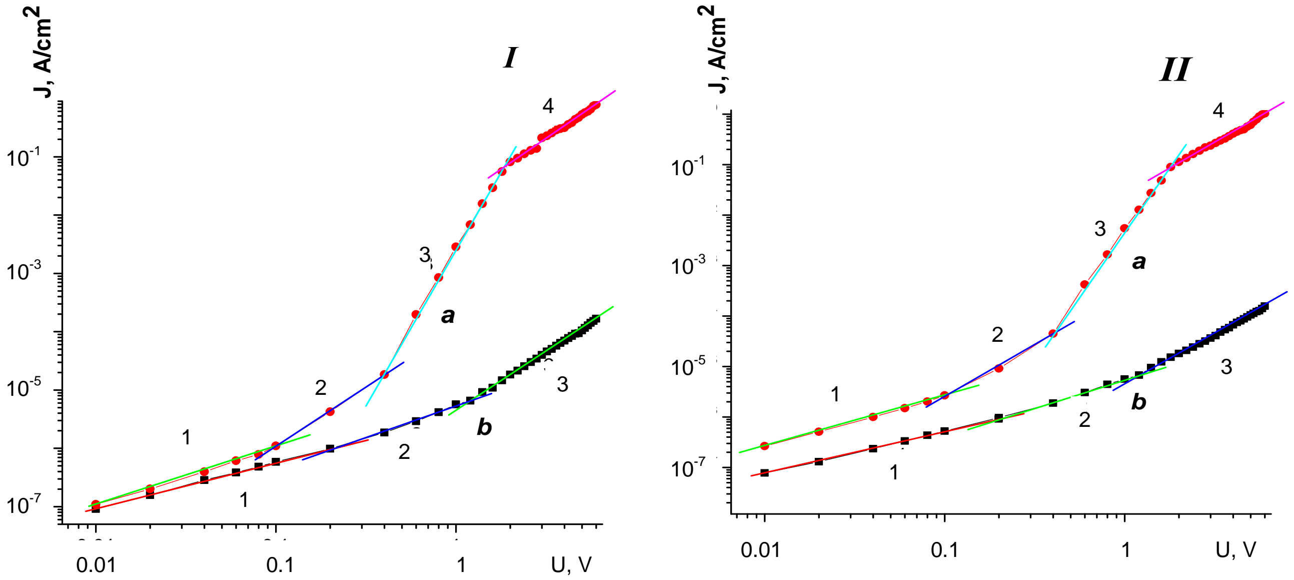

Fig. 5. Current-voltage characteristics of $J \sim U^{\alpha}$ type with different slopes in the forward (a) and reverse (b) current directions before (I) and after (II) UST. Ia: 1 (*1*), 2 (*2*), 5.3 (*3*), 2 (*4*). Ib: 0.84 (*1*), 1 (*2*), 2 (*3*). IIa: 1 (*1*), 2 (*2*), 5 (*3*), 2 (*4*). IIb: 0.79 (*1*), 1 (*2*), 2 (*3*).

as a result of which they cease to influence the magnitude of the surface potential.

Now, let us analyze the course of the dependence $D_{it}(\psi_S)$ obtained before the exposure to UST. As can be seen in Fig. 4a, the density of surface states at the interface of the $Al–Al_2O_3–p$-CdTe–Mo structure is sufficiently low, it is equal to $D_{it} = 3.4 \cdot 10^9$ cm^{-2}eV^{-1} at $\psi_S = 0$. The dependence of $D_{it}(\psi_S)$ in the lower and in the upper half of the forbidden band of semiconductor has a different pattern. For example, when ψ_S changes from 0 up to 0.17 eV, the density of surface states slowly decreases down to $\approx 2.4 \cdot 10^9$ cm^{-2}eV^{-1}, and then it rapidly increases and at $\psi_S = 0.18$ eV becomes equal to $D_{it} \approx \approx 5.7 \cdot 10^{10}$ cm^{-2}eV^{-1}. Then, its value decreases and at $\psi_S = = 0.23$ eV, reaches its minimum value equal to $\approx 1 \cdot 10^9$ cm^{-2}eV^{-1}. Then, the density of surface states begins to slowly decrease, and it becomes equal to $3 \cdot 10^9$ cm^{-2}eV^{-1} at 0.36 eV. Such a complex dependence $D_{it}(\psi_S)$ shows that the surface charges at the interface are non-uniformly distributed. The dependence $D_{it}(\psi_S)$ in the upper half of the band gap varies as follows. First, the density of surface states slowly decreases, and then rapidly increases and at $\psi_S \approx -0.22$ eV becomes $\sim 3 \cdot 10^{11}$ cm^{-2}eV^{-1}. In the upper half of the forbidden band of semiconductor, especially in the middle of the forbidden band, there is a non-uniform charge distribution in the space at the interface between the dielectric (oxide) and semiconductor. Now let us analyze the course of the dependence $D_{it}(\psi_S)$ after the impact of UST, which is shown in Fig. 4b.

The value of D_{it} in the lower half of the forbidden band after exposure to UST within the limits of the value $\psi_S = 0\ldots0.24$ eV decreases more than twice – from the value $\sim 7.6 \cdot 10^9$ cm^{-2}eV^{-1} down to the value $3.3 \cdot 10^9$cm^{-2}eV^{-1}, and then a peak appears at $\psi_S = 0.26$ eV and in it $D_{it} \approx 1.8 \cdot 10^{10}$ cm^{-2}eV^{-1}. Further, the D_{it}-value decreases relatively quickly to the value $\psi_S = 0.49$ eV, where it is $\sim 5.4 \cdot 10^9$ cm^{-2}eV^{-1}. After that, the density of surface states slowly decreases with a further increase with the surface potential, and at $\psi_S = 0.74$ eV reaches the value $\sim 1.9 \cdot 10^9$ cm^{-2}eV^{-1}.

In the upper half of the band gap, the value of $D_{it}(\psi_S)$ first increases to $\psi_S = -0.04$ eV, at which $D_{it} \approx \approx 2.4 \cdot 10^{10}$ cm^{-2}V^{-1}, then begins to decrease to $\sim 2.5 \cdot 10^9$ cm^{-2}V^{-1}, and then rapidly increases, and at $\psi_S \approx \approx -0.16$ eV it becomes equal to $2.6 \cdot 10^{11}$ cm^{-2}eV^{-1}. The above experimental results indicate that the oxide layer of Al_2O_3 formed between aluminum (Al) and cadmium telluride (CdTe) is of sufficient quality.

Apparently, UST annealing of surface states in the upper half of the forbidden band of semiconductor at the interface of the $Al–Al_2O_3–p$-CdTe–Mo structure leads to a decrease in the surface recombination current, and this, in turn, provides an increase in the number of injected electrons from aluminum to the base; therefore, an increase in the forward current after UST occurs. The decrease in the reverse current is due to the annealing of the surface states in the lower half of the forbidden band of semiconductor, since it decreases the probability of tunneling for non-equilibrium electrons accumulated at the interface from base to metal.

Since the Al_2O_3 oxide layer is the main element in the $Al–Al_2O_3–p$-CdTe–Mo structure under study, a change in its properties, including the concentration of defects and impurities in the dielectric-oxide layers (surface states), should affect the electrophysical and photoelectric properties of the entire structure. To confirm this assumption, the current-voltage characteristics of the structure in the forward and reverse directions before and after UST were investigated in [15] (Fig. 5).

The study shows that there is a power dependence of the current on the voltage type $J = AU^{\alpha}$, and the exponent α values before and after UST differ a little. It means that UST has almost no effect on the patterns of current flow in both the forward and reverse directions. At the same time, experimental results show that UST leads to an increase in current in the forward branch and to some decrease in the reverse branch of the *I–U* characteristic with the same offset voltage.

For example, the forward and reverse currents in the structure at the bias voltage $U = \pm 6$ V to UST are equal, $I_{forw} \cong 7.9 \cdot 10^5$ μA and $I_{rev} \cong 167.73$ μA, and their ratio at the same bias voltage (rectification coefficient) $K = 4707$. After UST, the above values for the same bias voltage value, respectively, become equal to $I_{forw} \cong 1.03 \cdot 10^6$ μA and $I_{rev} \cong 157.3$ μA, and $K = 6548$. It follows that the forward current increases by about 25…30%, and the reverse current decreases by 6…9%, the rectification coefficient (K) increases by 1.4 times after UST.

In conclusion, it can be noted that the MOS structure under investigation has a rather low density of surface states, especially in the lower half of the band gap of semiconductor. However, the dependence $D_{it}(\psi_S)$ in the lower and upper halfs of the forbidden band has different regularities. For example, the value of D_{it} in the lower half of the forbidden band after exposure to UST for the value $\psi_S = 0…0.24$ eV decreases more than twice from $\sim 7.6 \cdot 10^9$ down to $3.3 \cdot 10^9$ cm^{-2}eV^{-1}. UST substantially eliminates surface charge heterogeneity at the interface surface.

It has been ascertained that the annealing of surface states by means of UST exposure leads to an increase in the forward current by approximately 25…30% and to the decrease in the reverse current by 6…9%.

References

1. Baransky P.I., Belyaev A.E., Koshirenko S.M. et al. The mechanism of change in the mobility of charge carriers in the ultrasonic treatment of semiconductor solid solutions. *Fizika Tverdogo Tela*. 1990. **32**, No 7. P. 2159 (in Russian).
2. Ostrovskii I.V., Stelbenko L.P., Nadtochii A.B. Ultrasound-induced surface hardening of dislocation-free silicon. *Semiconductors*. 2000. **34**, No 3. P. 251–254.

Zaveryukhina E.B., Zaveryukhina N.N., Lezilova L.N. et al. Acoustostimulated expansion of the short-wavelength sensitivity range of AlGaAs/GaAs solar cells. *Techn. Phys. Lett*. 2005. **31**, No 1. P. 37–52.

4. Olikh O.Ya. Features of dynamic acoustically induced modification of photovoltaic parameters of silicon solar cells. *Semiconductors.* 2011. **45**. P. 798–804. https://doi.org/10.1134/S1063782611060170.
5. Davletova A., Karazhanov S.Zh. Open-circuit voltage decay transient in dislocation-engineered. *J. Phys. D: Appl. Phys*. 2008. **41**, No 16. P. 165107. https://doi.org/10.1088/0022-3727/41/16/165107.
6. Pashayev A.G. Effect of various treatments on Schottky diode properties *Semiconductors.* 2012. **46**, No 8. P. 1085–1087.
7. Mirsagatov Sh.A., Uteniazov A.K. The surface states of the Schottky diode with the structure-M(Al)-O(Al_2O_3)-S(CdTe). *Solid State Physics. XIII Intern. Sci. Conf.* Astana, Kazakhstan, 2016. P. 100–103.
8. Mirsagatov Sh.A., Uteniazov A.K. The density of surface states at the interface of the structure-M(Al)-O(Al_2O_3)-S(CdTe). *Doklady Akademii Nauk RUz*. 2016. No 5. P. 18–22.
9. Uteniazov A.K., Ismaylov K.A. The spectral distribution of the photosensitivity of the structure-M(Al)-O(Al_2O_3)-S(CdTe). *Materials of the Republican scientific-practical conference with the participation of foreign scientists*. Nukus, Uzbekistan. 2018. **1**. P. 45–48.
10. Mirsagatov Sh.A., Uteniyazov A.K. Injection photodiode based on *p*-CdTe film. *Techn. Phys. Lett.* 2012. **38**, No 1. P. 34–37. https://doi.org/10.1134/S1063785012010099.
11. Mirsagatov Sh.A., Muzafarova S.A., Baiev M.S., Achilov A.S. Study of the real structure of a Schottky Al–*p*-CdTe barrier diode. *Uzbek. Phys. Journal*. 2010. No 12. P. 154–168.
12. Achilov A.S., Zaveryukhin B.N., Kalanov M.U., Rustamov V.M. X-ray studies of the structure of a new type of A_2B_6 electromagnetic radiation receiver. *Doklady Akademii Nauk RUz*. 2014. No 2. P. 24–26.
13. Georgiou V.G. *Voltage-farad Measurements of Semiconductor Parameters*. Chisinau, Publ. House “Shtiints”, 1987.
14. Sze S.M., Ng Kwok K. *Physics of Semiconductor Devices*, 3rd Ed. Wiley, 2006.
15. Mirsagatov Sh.A., Uteniyazov A.K. Effect of ultrasound irradiation on the current-voltage characteristic of the Al–Al_2O_3–*p*-CdTe–Mo structure. *Doklady Akademii Nauk RUz.* 2018. No1. P. 21–24.

Uteniyazov Abatbay Kurbaniyazovich. Doctor of Physics and Mathematics (PhD), Associate Professor at the Department of Semiconductor Physics of Karakalpak State University, Uzbekistan, Nukus. Author of more than 40 scientific papers.

Ismailov Kanatbay Abdreymovich. Doctor of Physics and Mathematics, Professor, Head of Semiconductor Physics Department of Karakalpak State University, Uzbekistan, Nukus. Autor of more than 300 scientifical works, among them: 4 patents, 1 monograph, 10 text-books and educational-methodological manuals.